

## INVESTIGATING OF L-SHAPED SIDE SPILLWAY USING PHYSICAL AND NUMERICAL MODELLING OF CFD

**H. Souli    J. Ahattab    A. Agoumi**

*Hydraulic, Environmental Systems, Maritime, Soils and Structures, Hassania School of Public Works, Casablanca, Morocco, souli.hamza.cedoc@ehp.ac.ma jihaneahattab@gmail.com, agoumi.ali@gmail.com*

**Abstract-** The study is a comparison between physical and numerical modelling of side L shaped spillway using open-Foam. The particularity of this spillway is that the flow comes from two directions. In this paper, flow patterns are described in each part, and estimation for the water surface downstream the weir is given. The results shows that the numerical model fairly agrees with the outputs of the physical model with some deviations that can be explained by the high order of turbulence, perturbations and inflow conditions for high discharges. Afterwards we investigate 5 head discharges (1m, 2m, 3m, 4.8m, and 6.1m). The aim is to understand the behavior and the intermingling of the flow in the side channel trough. Furthermore, we study the flow patterns in the whole spillway and we compare the length of the water jet in the ski jump.

**Keywords:** L-Shaped Side Weir, Computational Fluid Dynamics (CFD), Hydraulic of Dams, Turbulence, VOF, and Spillway.

### 1. INTRODUCTION

Side channel spillways are hydraulic structures that collect water in lateral direction and leads it first to side channel trough opposite the crest and then turns approximately at the right angle and drops in the spillway chute (discharge channel), and finally goes to the structure of dissipation (the ski jump) Figure 1 [1-3].

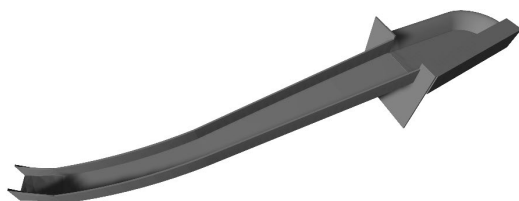


Figure 1. Example of side spillways with curved chute spillway

Classically, the flow in side spillways comes from one direction (lateral inflow), but for our study we consider a conception with two directions of flow (lateral and normal, Figure.2). The particularity of this conception is that we have the intersection of two plunging jet, thus it would be incorrect to assume that the lateral inflow has no impact on the side channel flow behavior or the water surface profile.

For the L shaped side spillway, the hypothesis of 1D flow trough will give us an underestimated water level inside the trough [4], [5], because in this approach we neglect the normal component of the flow for computing the water surface profile in the side channel trough. In this paper we try to model the side spillway using 3D numerical and physical approaches. The aim is to have a better understanding of the behavior of the flow in these types of structures and to estimate the water level in the side channel trough.

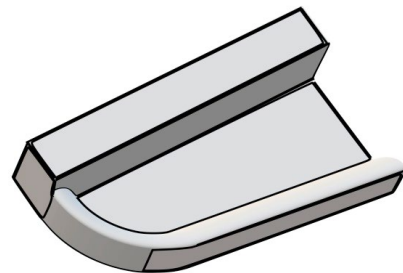


Figure 2. L-shaped side weir-flow directions

There have been numerous studies to investigate the flow on the side channel spillway published the first study on 1926 [1]. It focuses on the hydraulic performance of side channel. The authors of this publication tackle the problem using an experimental approach and introduce the equation of spatially varied flow. The same topic was introduced by [6] who describes with more detail the flow behavior inside the side channel trough with and estimation of the water surface level using linear momentum equations [6-8]. [4], [7] Compares the flow in side channel trough using 3 physical model and compares the experimental data with computational method using equation of the longitudinal surface profile [2,3], [8-10].

Despite the interest of this conception, there is no data or previous research available for the L-shaped side spillway. In this case we will use the experimental data collected from our physical model to validate our numerical model, in term of the water surface elevation and the flow patterns. Then we will try to give abacus for the water surface based on the comparison between physical and numerical methods. The objective is to predict the water elevation by discretizing the side channel trough to short reach  $\Delta_x$  and  $\Delta_y$ .

## 2. METHODS AND MODELLING

### 2.1. Water Surface Estimation

The conservation of linear momentum is used to calculate the water surface in side channel weir [6]. It is known that side channel plays a role of dissipator of hydraulic energy that comes from the crest of the weir through mixing with the channel flow.

$$\Delta_y = \frac{Q_2(V_1+V_2)}{g(Q_1+Q_2)} \left[ (V_1+V_2) + \frac{V_1(Q_2-Q_1)}{Q_1} \right] \quad (1)$$

In side channel spillways, we always try to establish a control section in order to increase the upstream depths, so the channel can be made to flow at subcritical regime. The objective is to avoid intermingling [6], high energy transverse, violent wave action, high order of turbulence and vibrations that can cause damage to the hydraulic structure [5], [11-13].

### 2.2. Numerical Model

The 3D geometry of the spillways was prepared using the free software FreeCAD [14]. We used the ogee profile for the conception of the weir with the height difference between the weir level and its bottom varying from 15 m to 20 m. The side channel has a trapezoidal cross section with a slope of 5% and at the end; there is transition into rectangular section that continues until the control section. The length of the linear part of the weir is 75 m and the curved part is 55 m. The width of the side channel trough is varying from 21 m at the beginning to 36 m at the control section. The length of the side spillway chute is about 300 m, and it contains a curvature of a radius  $R=400$  m at the upstream of the ski jump, Figure 1. To investigate the flow patterns, the water surface profile and the behavior of the flow in each part of our spillway. Constructing the numerical model involves numerous sequential stages [15], [16].

- Post Pre-Processing: drawing geometry; grid generation, turbulence model, boundary conditions and implementing the initial conditions.
- The Solver: its objective is to solve the continuity and momentum equations coupled with some additional models in order to close the system and guarantee convergence, stability and accuracy. The post processing: visualization of the outcomes (velocity field, pressure, water surface)

#### 2.2.1. Post Pre-Processing

The model was implemented using Open-FOAM [17] which is a free software that can solve a wide range of problem in relation with continuum mechanics, and especially in fluid dynamics. The method of finite volume is used to obtain the algebraic equations after discretizing the domain into small control volumes and then we integrate over this control volume in order to obtain discretized equations that can be solved using iterative methods. The software solves the Reynold Navier -stokes equations (RANS) using the function volume of fluid VOF (Volume of Fluid) in order to define the free surface flow.

#### 2.2.2. Mesh Sensitivity Analysis

Concerning the geometry, we use the FreeCAD software with the purpose of drawing the shape of the arced weir, the collecting trough and the complete spillway using the format STL (stereolithography). For the meshing, we use the command blockMesh [18] and snappyHexMesh in Openfoam in order to mesh our geometry. The snappyHexMesh tool automatically generates three meshes comprising of hexahedra and split-hexahedra from triangulated surface geometries or tri-surfaces provided in STL format. After that, we use the setFields utility that helps us set initial water level.

To ensure the appropriate mesh size was chosen for each case study, a grid sensitivity analysis was conducted, incorporating different mesh sizes. In the case of the entire side spillway with a curved chute, three grid sizes were employed: 0.5 m, 0.2 m, and 0.1 m. and we found that the proper mesh is 0.2 m, Table 1. The total number of meshes varies between 2 250 663cells and 18 360 599. The Table 1 summarizes the tested cases with the size and number of cells for each case tested.

Table 1. Mesh convergence analysis

Location	H (m)	Cell size (m)	Total number of cells
The whole spillway	1 m, 2 m, 3 m, 4 m, 4.8 m, 6.1 m	0.5 m	3 530 259
		0.2 m	8 450 235
		0.1 m	18 360 599
Arc side weir + The side channel trough	1 m, 2 m, 3 m, 4 m, 4.8 m, 6.1 m	0.2 m	2 250 663

The choice was justified by the fact that the shape of the water surface and the hydraulic parameters values are the closest to the measured values in the physical model in terms of flow patterns, velocity, pressure and cavitation.

#### 2.2.3. Turbulence Model

The turbulence modelling approach adopted (RANS or LES) as well as the turbulence model chosen. In this project, we did a sensitive approach in order to choose the best model of turbulence that have a good agreement with experimentations. After a sensitive analysis about the choice of turbulence models, we select  $k-\omega$ SST as model of turbulence for our simulation. The water surface can be estimated by a plethora of interface capturing methods. The volume of fluid method is one of the most methods used to capture the water surface. The VOF method employs the fraction function  $\alpha$  as an indicator to determine the proportion of the cell occupied by water, air, or both. The resolution of these governing equations (3-10) gives the velocity, pressure field and the tracking of water surface. The equations that govern the system are as follows:

$$\frac{\partial k}{\partial t} + \frac{\partial k u_i}{\partial x_i} - \frac{\partial}{\partial x_i} (\mu_{keff} \frac{\partial k}{\partial x_i}) = \min(G, c_1 \beta k \omega) - \beta^* k \omega \quad (2)$$

$$\frac{\partial \omega}{\partial t} + \frac{\partial \omega u_i}{\partial x_i} - \frac{\partial}{\partial x_i} (\mu_{keff} \frac{\partial \omega}{\partial x_i}) =$$

$$= \gamma_i \min(S_2, \frac{c_1}{a_1}) \omega \max(a_1 \omega, b_1 F_{23} \sqrt{S_2} - 1) CD_{k\omega}$$

$$\mu_{keff} = \alpha_{ki} v_t + \nu \tag{4}$$

$$\mu_{\omega eff} = \alpha_{\omega i} v_t + \nu \tag{5}$$

$$v_t = \frac{a_1 k}{\max(a_1 \omega, b_1 F_{23} \sqrt{S_2})} \tag{6}$$

$$S_{ij} = \frac{1}{2} \left( \frac{\partial u_j}{\partial x_i} + \frac{\partial u_i}{\partial x_j} \right) \tag{7}$$

$$S_2 = 2 S_{ij} S_{ij} \tag{8}$$

$$G = v_t S_{ij} S_{ij} \tag{9}$$

$$CD_{k\omega} = 2 \alpha_{\omega 2} \frac{\partial k}{\partial x_i} \frac{\partial \omega}{\partial x_i} \frac{1}{\omega} \tag{10}$$

where,  $k$  is turbulent kinetic energy,  $\omega$  is the turbulent specific energy dissipation rate  $u_i$  is velocity component in the direction of  $x_i$ ,  $\mu_{keff}$  and  $\mu_{\omega eff}$  are the effective diffusivity for  $k$  and  $\omega$ , respectively,  $v_t$  is the turbulent kinetic viscosity,  $\nu$  is the kinematic viscosity,  $G$  is the production of turbulence due to shear,  $S_{ij}$  is the strain-rate tensor.

The subscript can be either 1 or 2 depending on the blending function. The constant:

where,  $\alpha_{k1}, \alpha_{k2}, \alpha_{\omega 2}, \alpha_{\omega 1}, a_1, b_1, c_1, \beta^*, \gamma_1, \gamma_2$  is equal to 0.85, 1, 0.5, 0.856, 0.31, 1, 10, 0.09, 5/9, 0.44, and  $F_1$  and  $F_{23}$  are blending functions.

### 2.3. Construction of the Physical Model

The physical model for this study is a 3D model in order to observe the effect of 3D conditions, and to have a better idea about the flow behavior at the inlet of our hydraulic structure, at the side trough, the spillway chutes and at the dissipator part. The experimental facility includes:

The upstream portion is comprised of a rectangular basin measuring 15 meters by 20 meters. Additionally, a rectangular basin forms the downstream section, which is dedicated to studying the issue of scour. However, the details of this downstream section are beyond the scope of the current article. Instrumentation:

- High-precision rolling point instruments were employed to measure the flow height above the weir, with an accuracy of  $\pm 1$  mm.
- A magnetic flow meter was utilized to measure the flow rate with a precision of  $\pm 0.5\%$ .
- The velocity was measured using a Pitot tube with an accuracy of  $\pm 0.1\%$ .

The physical model of the spillway was developed based on the principle of Froude similitude.

$$F_r = \frac{V}{\sqrt{gh}} \tag{11}$$

With the objective of examining the flow patterns and the configuration of the water surface, thorough investigations were conducted. A model with a scale of 1/55 was built; this model helps the visualization of the flow in each part of the side spillway. Five different discharges were tested ranging from (1 m to 6.1 m).

For each aspect of the current research, laboratory data samples will be provided for comparative analysis alongside the numerical approaches employed. To measure the water level in the collection trough, we have installed more than 30 water level sensors. Our aim is to compare the measured water levels with those calculated numerically. These sensors are located at the same points as those calculated numerically by the software (Figure 5).

### 3. RESULTS AND DISCUSSION

The calculation time taken for this simulation was 21 hours for each head discharge and 60 hours for the whole spillway using eight core processors. The results were post-processed using the ParaView software, which allows the visualization of pressure and velocity fields inside the domain, the extraction of streamlines and the monitoring of the evolution of the water level.

#### 3.1. Calibration

The discharge capacity of a spillway with crest weir is given by the following formula:

$$Q_{th} = CLH^{1.5} \tag{15}$$

The comparison between the numerical and theoretical calculations concerns specifically the discharge head above the weir and in the control section. The Table 2 summarizes the difference.

Table 2. Calibration of the model using physical model

H head discharge (m)	Q (Th)	Q max (OpenFoam)	Q avg (OpenFoam)	Q Physical model
2	718	785	731	702
3	1382	1498	1317	1356
4.8	2974	3066	2728	2890

Upon analyzing the outcomes, it is evident that the maximum relative deviation between theoretical and numerical values does not surpass 10%. Additionally, this deviation tends to decrease further for high head discharges. In macro way, we can justify these differences between the numerical and theoretical values by the fact that the latter are derived from analysis on several physical models where the flow is closer to reality, yet the numerical values are obtained from the discretized resolution of Navier -stokes equations, which implies several simplifying hypotheses of calculation.

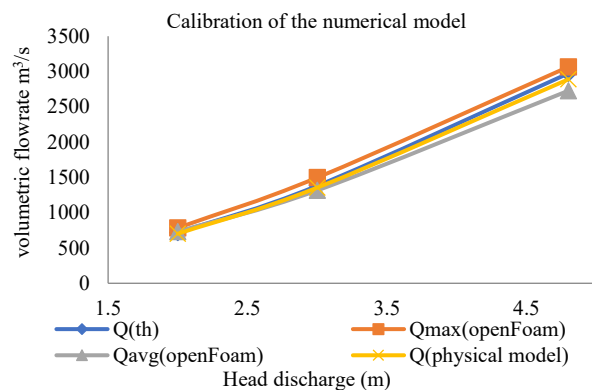


Figure 3. Calibration of the numerical method

### 3.2. Water Surface in the Side Channel Trough

In this section, we calculate the water level for  $H=4.8$  m above the weir of the side channel trough using the formula from the design of small dams [19]. The calculation results of the water slide in the receiving trough are given in the Table 3.

Table 3. Theoretical calculations of water surface in side channel trough

$X$ (m)	$B$ (m)	$\Delta y$ (m)	$h$ (m)
92	36	-	13.8
86.11	35.86	0.17	13.76
81.11	34.32	0.17	13.68
76.11	33.85	0.18	13.61
71.11	32.43	0.17	13.54
66.11	31.9	0.16	13.46
61.11	31.14	0.15	13.37
56.13	30	0.14	13.28
51.11	29.23	0.13	13.18
46.12	28	0.13	13.07
41.11	27.65	0.12	12.96
36.11	26.4	0.1	12.84
31.11	25.8	0.1	12.72
26.11	24.61	0.09	12.59
21.11	23.2	0.09	12.45
16.11	22.05	0.08	12.29
11.14	21.93	0.05	12.12
6.11	21.5	0.06	11.93
2.81	21	0.02	11.78

The theoretical results shown in the Table 4 that the water surface profile is underestimated in comparison with results of experimental data and numerical modelling due to the neglecting of the contribution of the frontal part. The maximum water level computed using the theoretical method is 13.8 m whereas in both CFD and physical model is more than that. Due to the contribution of the frontal part in the side channel trough there is more aeration and turbulence in comparison with the classic side weir. It is recommended for this type of structure to use CFD methods instead of theoretical calculations for the initial design and validate it using experimental methods.

### 3.3. Control Section

The aim of the implementation of the control section in the side channel trough is to create a subcritical flow, this regime will increase the flow depth and decrease the velocities, because the fall of water coming from the L shaped side weir will face a low drop. It is necessary to choose the geometrical parameters (slope, trapezoidal section, ogee crest height) wisely in order to guarantee a subcritical regime in the channel, in the objective to avoid high level of intermixing and turbulence of the energy transverse flow with the channel stream.

For this type of conception, the side channel trough plays a major role of dissipation of the hydraulic energy. The creation of the control section downstream the side channel trough can be achieved by raising the bottom of the trough by 1m for our project. The height of water in this section is equal to the critical depth  $h_c$  specified using Equation (16) [2].

$$h_c = \sqrt[3]{\frac{Q^2}{gB^2}} \tag{16}$$

The comparison between the experimental, numerical and theoretical calculation concerns specifically the height of water in the control section downstream of the trough for the design head ( $H=4.8$  m). The Table 4 summarizes the differences:

Table 4. The height of water in the control section downstream of the trough for the discharge of the project  $H=4.8$  m

physical model (m)	theoretical calculations (m)	Open-FOAM (m)
8.9	8.85	8.7

This Table shows that on the control section downstream the side channel trough; the results of experimental data, theoretical and CFD show a good agreement in terms of the height of the water level in this section.

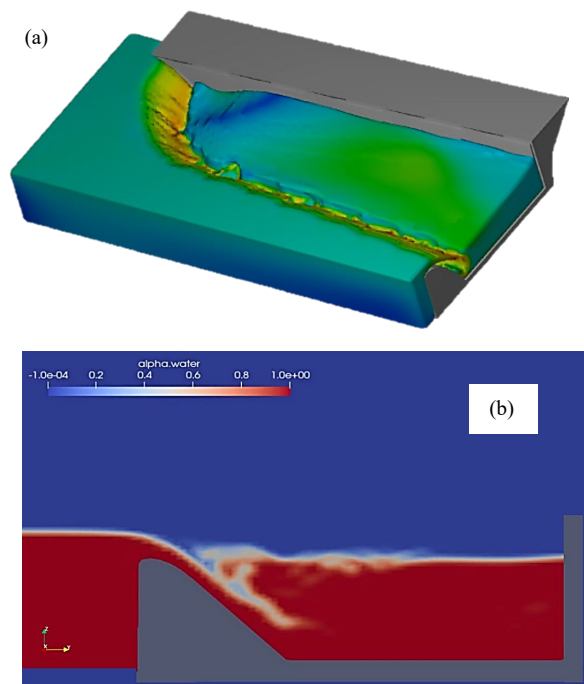


Figure 4. Example of simulation of side channel trough using Open Foam for the discharge of the project, a)  $H=4.8$  m, b)  $H=6.1$  m

This verification ensures that the numerical approaches can give similar flow patterns and numerical values as the physical model. The numerical modelling underestimates the height of water in this section in comparison with theoretical calculations and physical model (Table 5).

### 3.4. Longitudinal Water Surface Profiles

In order to be able to deduce an estimation law of the flow surface that could be applied to other project with the same magnitude of the flow rate, and with the same geometry conditions, we used a dimensionless variables

$$X \text{ and } Y, \text{ with } X = \frac{x}{L} \text{ and } Y = \frac{y}{L} \text{ (Figure 5).}$$

The calculation process consists of the following steps:

- Perform the numerical simulation in the side channel trough for different discharges head starting from 1m to 6.1 m.

- Take longitudinal sections for the following portions 27%, 34%, 41%, 48%, 56%, 63%, 70%, 77% and 84%.
- The origin of the reference is located downstream the side channel trough.
- For each longitudinal section, the water depth is estimated from the downstream section of our geometry for different discharges.

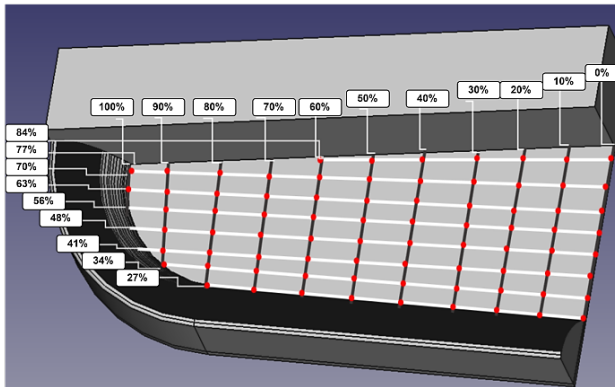


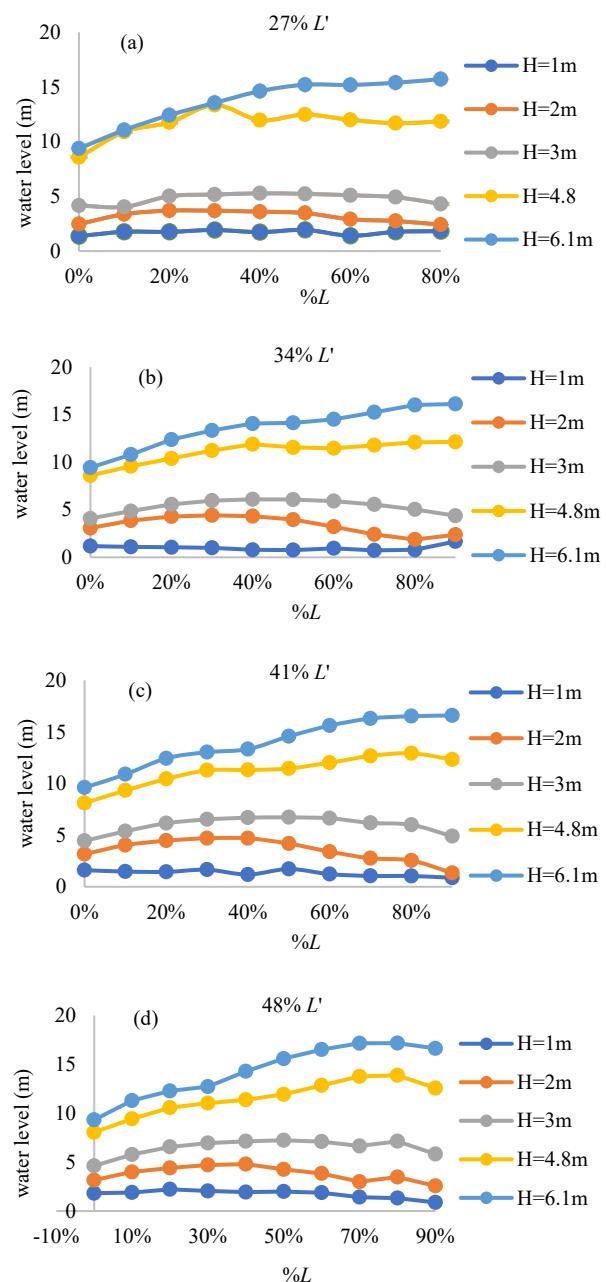
Figure 5. Discretizing the side channel into longitudinal sections

The selection of these portions is based on observation in the reduced model. We chose these portions to try to find an explanation for the bump forming at the collector trough due to the two directions of the flow and to understand the shock waves [20]. We divided the collector trough into several profiles in order to capture all the perturbations and water levels in this specific zone. As far as we know, no previous research had investigated the L-shaped side spillway using the comparison between experimental data and the numerical approaches. The aim of this part is to develop a generalizable law of water surface in the side channel trough using the combination of numerical and experimental tools. These laws will help the designers and hydraulic engineers to have an idea about the flow for their initial design for project with the same magnitude of discharges.

The simulation of the flow in the side channel trough showed the appearance of shock waves and vortices due essentially to the abrupt change in the direction of the flow coming from the two directions (lateral and normal). At relatively small discharge ( $H=1$  to  $2$  m) the flow depth in the side channel is small and we observe the formation of dissymmetric vortex and streamlines because the linear part (lateral) feeds the flow more than the curved part (normal). For high discharge ( $H=3$  to  $6.1$  m) the superposition of the two plunging jet causes fluctuations of the water surface (Figures 7 and 8) along the side channel trough with a chaotic motion of the water surface and the formation of vortices in all directions. The Figures 6a-6i show the longitudinal section of the flow in the side channel trough using numerical approaches. Where,  $L$  is the total longitudinal length of the side channel trough and  $L'$  the length of the transverse section (curved part). All the figures of the water surface are in percentage, for each graph, we fix the transverse section and we vary the longitudinal sections:

For the section  $Y=27\%$ :

The water level remains constant with small fluctuations for ( $H=1$  to  $3$  m). For high discharge ( $H=3$  to  $6.1$  m) the profile of water raises quickly, with the increase of the flow rate that causes vortices in all direction and perturbations. The maximum height is  $16$  m (Figure 6a). For the section varying from  $Y=34\%$  to  $63\%$ , the water surface is varying gradually with moderate fluctuations for small head discharges up to  $3$  m above the side weir. For high flow rate, the depth of water soars steeply and reached  $16$  m as maximum height (Figures 6b-6f). For  $Y$  starting from  $70\%$  to  $84\%$ , the surface of water climbs significantly even for small discharges,  $10$  m as maximum height for small discharges and reached  $20$  m for high flow rates. The rise in water level observed in these longitudinal sections can be attributed to the formation of local perturbations. Because the linear part (lateral) feeds more the flow than the curved part (normal component of the flow).



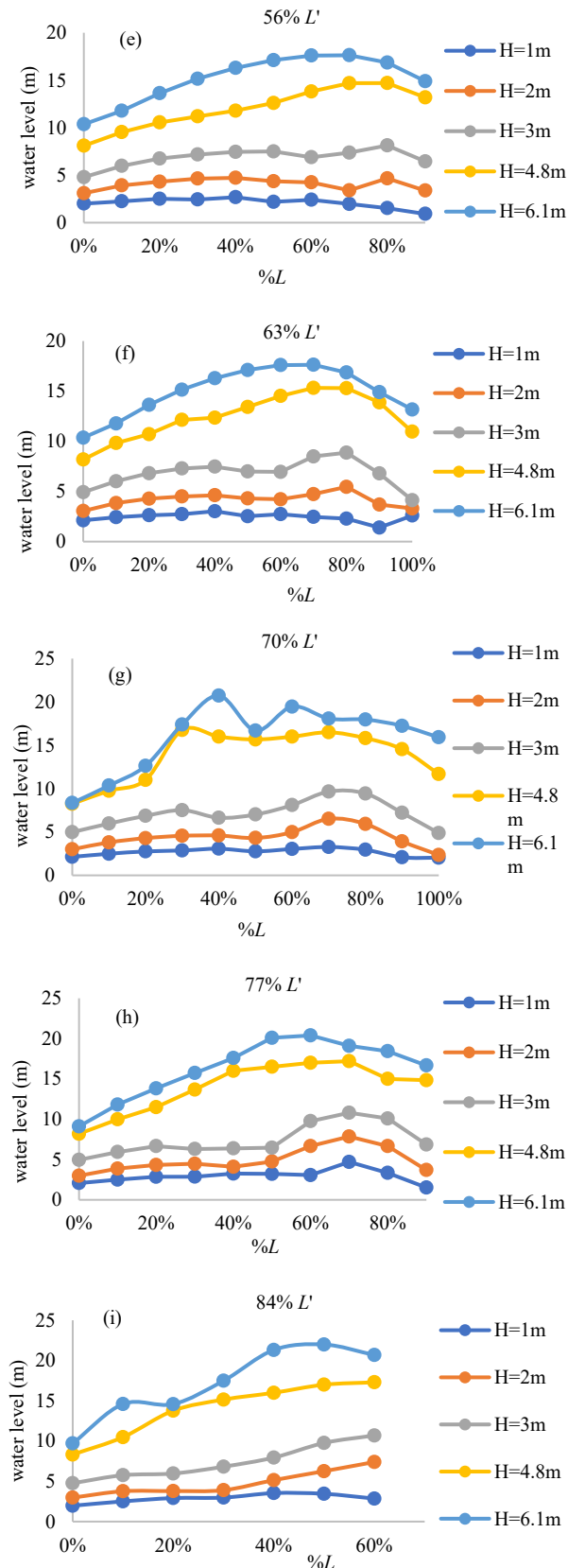


Figure 6. Surface of water inside the side collector trough for different discharges ( $H=1\text{ m}$ ,  $2\text{ m}$ ,  $3\text{ m}$ ,  $4.8\text{ m}$ ,  $6.1\text{ m}$ )

This local perturbation is formed between (30% to 60% along  $X$  direction), and after passing the 60% along  $X$ , this perturbation is damped and dissipated (Figures 7-8) with the flow, until it reaches the control section where the water level goes down to reach 8.8 m. The pictures taken from the physical model illustrate the formation of vortices in all directions and shock waves (Figures 7-8). These water surfaces are (prototype) i.e. multiplied with the scale (applying the similitude theorem).

For small discharges:



Figure 7. Flow patterns in physical model for small discharge ( $H=2\text{ m}$ )

For high discharges:

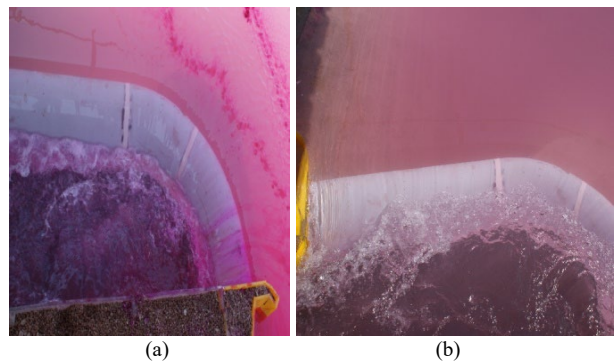


Figure 8. Flow patterns in physical model for small discharge a)  $H=4.8\text{ m}$ , b)  $H=6.1\text{ m}$

In this section, we compare the water level in the side channel trough using both numerical and physical model for different percentage of  $L'$  (27 %, 48%, 63%, 70%). Overall, the comparison shows a good agreement between the values derived from experimentation and Open FOAM. The difference between the two tools can be explain by the rate of air transport, the water surface is inflated in the physical model as in the numerical approaches. Shock waves in the collector trough generate a lot of air that is underestimated by numerical modelling. The comparison between CFD and experimentation in percentage shows that the relative error does not exceed 15 % (Figure 10).

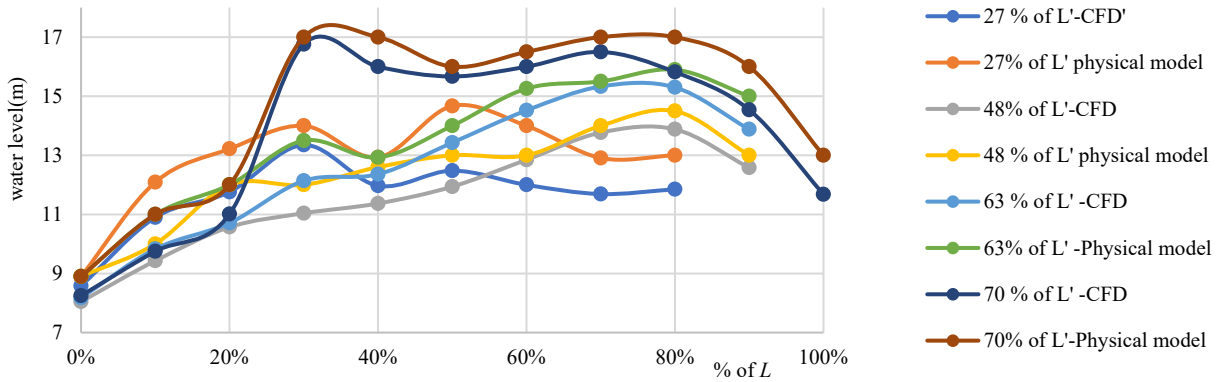


Figure 9. Comparison between physical model and open-FOAM for the head discharge of the project for  $Y=27\%$ ,  $48\%$ ,  $63\%$ ,  $70\%$

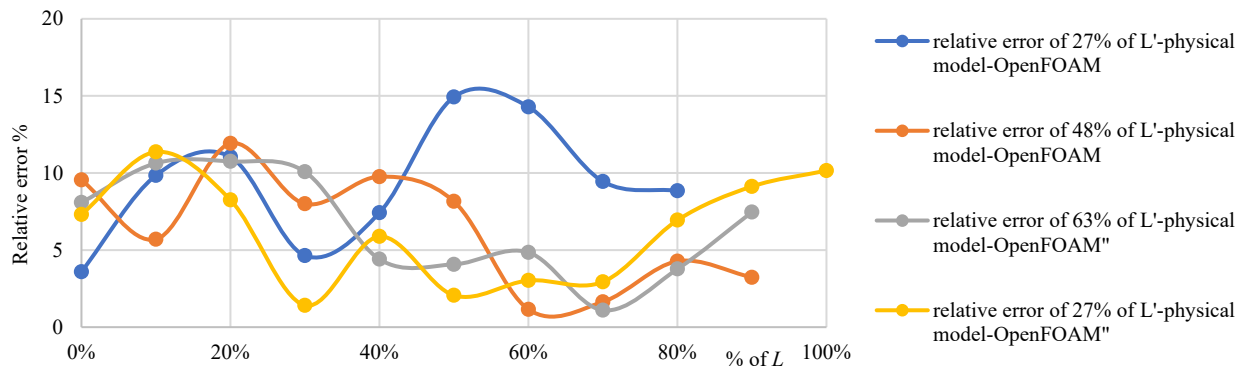


Figure 10. Comparison of the RME (Relative Mean Error) using CFD and physical model for the discharge of the project ( $H=4.8$  m) for  $Y=27\%$ ,  $48\%$ ,  $63\%$ ,  $70\%$

### 3.5. Side Spillway

The aim is:

- To visualize the flow patterns after the side channel trough.
- Analyze the flow behavior for the discharge head of the project.
- To compute the distance of the jet downstream, the ski jumps and compare it with the physical model.

In order to have a better understanding of the flow behavior along the side spillway we used 2 million in terms of the mesh resolution, therefore the execution of the simulation took approximately 18 hours with 8 processors. We have chosen 0.8m for the mesh size in the side channel trough and 0.9 m in the spillway chute and ski jump. These mesh sizes provide a good compromise between an acceptable simulation time and good accuracy that provides the desired results. The results of the 3D modelling, shown in the Figure 11 give a clear visualization of the flow in steady state in the whole side spillway and downstream the ski jump. The figure illustrate that the water jet takes off over the entire ski jump even with the existence of the curvature upstream the ski jump. This result is very important, because it shows that the water jet does not jeopardize the stability of the structure. The Table 5 summarizes the empirical (physical model), theoretical and numerical values of the jet range  $D$ :

Table 5. The length of the jet downstream the dam

$D$ (physical model) (m)	$D(th)$ (m)	$D(num)$ (m)
96	75	93

The distance from the spillway to the impact point of the water jet seems to be considerable and far from the dam. The measured water jet downstream the ski jump in the physical model is close to the numerical value, consequently, the findings indicate that numerical approaches can be utilized to estimate the water jet for structures of this nature. To have an idea about the distance at the phase of initial design is very important, because it will give an idea about the measure that can be done in order to ensure the safety of the dam.

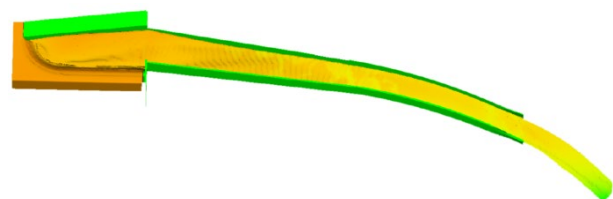


Figure 11. Simulation of the side spillway for the discharge of the project  $H=4.8$  m- global view of the side channel spillway with the water jet in the ski jump

### 4. CONCLUSION

In this paper, the influence of the L-shape side weir was investigated using computational fluid dynamics CFD and experimental results, with different discharges starting with  $H=1$  m to  $H=6.1$ . The analysis leads to the following conclusions:

- The L-shaped side spillway contains high degree of turbulence, vibrations, roster tails in comparison with the classic side weir with one lateral direction of the flow.

- The flow inside side channel trough is characterized by formation of vortices in all directions for high discharges unlike the standard side channel, which have less vortex (single, two or tornado vortex).
- $K-\omega$  *sst* model as closed model for turbulence can predict fairly the flow patterns in L-shape side spillway.
- The water level increase for the L-shape side channel in comparison with the classic side spillway due to the presence of the second direction flow. The perturbation on the side channel trough will depend essentially on the length of the two directions.
- It is recommended that a maximum of 2/3 submergence in the side channel trough can be tolerated. As the degree of submergence increases the discharge coefficient must be reduced until saturation.
- The abacus given in this paper will help hydraulic designers for this type of structure that have the same magnitude of flowrate (2950 m<sup>3</sup>/s equivalent of  $H=4.8$  m) to estimate the water level at the phase of initial design, but for the final conception they must take into consideration the topographic, geotechnical issues and to validate the hydraulic performance, a physical model was employed at an appropriate scale to mitigate any potential scale effects.
- The objective of simulating the side spillway is to gain insights into the flow characteristics within the chutes and ski jump, as well as to assess the distance covered by the water jet.

The present paper highlights several points in the study of the L shape side spillway, including the description of the flow patterns in the side channel trough, comparison between theoretical, experimental and numerical tools. Additionally, it provides a reference table for water levels, enabling the estimation of geometrical parameters for the side arced weir and side collecting trough in projects with similar head discharge magnitudes.

## NOMENCLATURES

### Symbols / Parameters

- $\Delta_y$  : The decrease in water surface elevation over the length of the channel, denoted as  $\Delta_x$   
 $g$  : The acceleration of gravity equal to 9.8 m/s<sup>2</sup>  
 $Q_1, Q_2$  : Flows discharged by weir between successive sections 1 and 2 in (m<sup>3</sup>/s)  
 $V_1, V_2$  : Velocities in sections 1 and 2 respectively in m/s  
 $U_e$  : The entrance velocity  
 $I$  : Turbulence intensity ranging from 2% to 10%  
 $L$  : Scale of turbulence  
 $Q_{th}$  : Value derived from theoretical calculations (m<sup>3</sup>/s)  
 $Q_{max}$  (OpenFoam) : Value derived from numerical methods (maximum value) (m<sup>3</sup>/s)  
 $Q_{avg}$  (OpenFoam) : Value derived from numerical methods (average value) (m<sup>3</sup>/s)  
 $Q$  (Physicalmodel) : Value derived from the physical model (m<sup>3</sup>/s)

- $X$  : The variation along longitudinal axis  
 $h$  : Water level  
 $B$  : The variation of the width of section in side channel trough  
 $Q$  : The total discharge (m<sup>3</sup>/s)  
 $h_c$  : The critical height in (m)  
 $D(num)$  : Value derived from numerical simulation in m  
 $D(physicalmodel)$  : Value derived from physical model in m  
 $D(th)$  : Value derived from theoretical formula in m  
 $V$  : Flow velocity  
 $g$  : Gravity constant  
 $h$  : Flow depth  
 $\rho$  : Water density  
 $\sigma$  : Water surface tension  
 $\nu$  : Water kinematic viscosity  
 $k$  : Turbulent kinetic energy  
 $\omega$  : THE turbulent specific energy dissipation rate  
 $u_i$  : Velocity component if the direction of  $x_i$   
 $\mu_{keff}$  : Effective diffusivity for  $k$   
 $\mu_{\omega eff}$  : Effective diffusivity for  $\omega$   
 $\nu_t$  : Turbulent kinetic viscosity  
 $G$  : Production of turbulence due to shear  
 $S_{ij}$  : Strain-rate tensor.  
 $F_1$  and  $F_{23}$  : Blending functions  
 $C$  : Discharge coefficient  
 $H$  : Head discharge  
 $h_c$  : Critical depth  
 $L$  : Width of the spillway

## ACKNOWLEDGEMENTS

The authors sincerely thank the Moroccan hydraulic laboratory. Special thanks go to Hassania School of public works in Casablanca, Morocco.

## REFERENCES

- [1] J. Hinds, "Side Channel Spillways: Hydraulic Theory, Economic Factors, and Experimental Determination of Losses", Trans. Am. Soc. Civ. Eng., Vol. 89, No 1, pp. 881-927, 1926.
- [2] B. Perry, "Open-Channel Hydraulics. Ven Te Chow. McGraw-Hill, New York, 1959. xviii + 680 pp. Illus. \$17", 1959, Science, Issue 3408, Vol. 131, p. 1215, April 1960.
- [3] D. Vischer, W.H. Hager, "Dam Hydraulics", Wiley Chichester, Vol. 2, pp. 57-62, 1998.
- [4] J. Lucas, N. Lutz, A. Lais, W.H. Hager, R.M. Boes, "Side-Channel Flow: Physical Model Studies", J. Hydraul. Eng., Vol. 141, No. 9, p. 05015003, 2015.
- [5] R. Reinauer, W.H. Hager, "Supercritical Bend Flow", J. Hydraul. Eng., Vol. 123, No. 3, pp. 208-218, 1997.
- [6] U.S.B. of Reclamation, "Design of Small Dams", US Department of the Interior, Bureau of Reclamation, pp. 353-354, 1987.



- [7] W.H. Hager, A.J. Schleiss, R.M. Boes, M. Pfister, "Hydraulic Engineering of Dams", CRC Press, pp. 20-35. 2020.
- [8] V.H. Vayghan, M. Mohammadi, A. Ranjbar, "Experimental Study of the Rooster Tail Jump and End Sill in Horseshoe Spillways", Civ. Eng. J., Vol. 5, No. 4, pp. 871-880, 2019.
- [9] H. Chanson, M. Pfister, "Scale Effects in Modelling Two-Phase Air-Water Flows", The 35th IAHR World Congress, TPU pp. 1-10, 2013.
- [10] S. Erpicum, B.P. Tullis, M. Lodomez, P. Archambeau, B.J. Dewals, M. Pirotton, "Scale Effects in Physical Piano Key Weirs Models", J. Hydraul. Res., Vol. 54, No. 6, pp. 692-698, 2016.
- [11] M. Ghaeini Hesaroyeh, A. Tahershamsi, M.M. Namin, "Numerical Modelling of Supercritical Flow in Rectangular Chute Bends", J. Hydraul. Res., Vol. 49, No. 5, pp. 685-688, 2011.
- [12] R. Reinauer, W.H. Hager, "Supercritical Flow in Chute Contraction", J. Hydraul. Eng., Vol. 124, No. 1, pp. 55-64, 1998.
- [13] R. Reinauer, W.H. Hager, "Supercritical Flow Behind Chute Piers", J. Hydraul. Eng., Vol. 120, No. 11, pp. 1292-1308, 1994.
- [14] B. Falck, D. Falck, B. Collette, "Freecad [How-To]", Packt Publishing Ltd., p. 10, 2012.
- [15] D.C. Wilcox, "Turbulence Modeling for CFD", DCW Industries La Canada, Vol. 2, pp.100-150, Canada, 1998.
- [16] S. Rodriguez, "Applied Computational Fluid Dynamics and Turbulence Modeling", Springer, pp. 100-300, 2019.
- [17] C.J. Greenshields, "OpenFOAM User Guide", OpenFOAM Found. Ltd Version, Vol. 3, No. 1, p. 47, 2015.
- [18] P. Lopes, "Free-Surface Flow Interface and Air-Entrainment Modelling Using OpenFOAM", Ph.D. Thesis, pp. 50-100, 2013.
- [19] W. Duncan, C. Huntley, J. Hokenstrom, A. Cudworth, T. McDaniel, "Design of Small Dams - A Water Resources Technical Publication, Final Report", Bureau of Reclamation, Engineering and Research, pp. 353-354, Denver, USA, 1987.
- [20] H. Souli, J. Ahattab, A. Agoumi, "Investigating Supercritical Bended Flow Using Physical Model and CFD, Model. Simul. Eng., Vol. 2023, p. 5542589, March 2023.

## BIOGRAPHIES



**Name:** Hamza  
**Surname:** Souli  
**Birthdate:** 16.03.1994  
**Birthplace:** Casablanca, Morocco  
**Bachelor:** Hydraulics and Environment, Department of HEC, Hassania School of

Public Works, Casablanca, Morocco, 2015  
**Master:** Hydraulics and Environment, Department of HEC, Hassania School of Public Works, Casablanca, Morocco, 2018  
**Doctorate:** Student, Hydraulic/CFD, SHEMASS, Hassania School of Public Works, Casablanca, Morocco, Since 2020  
**Research Interests:** Hydraulics, CFD, Fluid Mechanics, Environment  
**Scientific Publications:** 1 Paper, 1 Book



**Name:** Jihane  
**Surname:** Ahattab  
**Birthdate:** 18.03.1988  
**Birthplace:** Marrakech, Morocco  
**Bachelor:** Hydraulics and Environment, Department of HEC, Hassania School of Public Works, Casablanca, Morocco, 2008  
**Master:** Hydraulics and Environment, Department of HEC, Hassania School of Public Works, Casablanca, Morocco, 2010  
**Doctorate:** Hydrology and Environment, Department, Faculty of Sciences Semlalia, University Cadi Ayyad, Marrakech, Morocco, 2016  
**The Last Scientific Position:** Assist. Prof., Department HEC, Ecole Hassania des Travaux Publics, Casablanca, Morocco, Since 2017  
**Research Interests:** Hydraulics, Hydrology, Environment  
**Scientific Publications:** 6 Papers, 1 Book



**Name:** Ali  
**Surname:** Agoumi  
**Birthdate:** 29.01.1958  
**Birthplace:** Fes, Morocco  
**Bachelor:** Civil Engineering, School of Bridges and Roads, Paris, France, 1978  
**Master:** Civil Engineering, School of Bridges and Roads, Paris, France, 1980  
**Doctorate 1:** Civil Engineering, School of Bridges and Roads, Paris, France, 1982  
**Doctorate 2:** Oceanography, University of Paris 6, Paris, France, 1985  
**The Last Scientific Position:** Prof., Department of HEC, Hassania School of Public Works, Casablanca, Morocco, Since 1986  
**Research Interests:** Environmental Engineering, Ecological Engineering, Civil Engineering, Water Science, Irrigation and Water Management, Environmental Science  
**Scientific Publications:** 20 Papers, 10 Chapters, 1 book